Eur Biophys J (2003) 32: 128–136
DOI 10.1007/s00249-002-0275-6

ARTICLE

**María Tirado-Miranda · Artur Schmitt**
**José Callejas-Fernández · Antonio Fernández-Barbero**

# The aggregation behaviour of protein-coated particles: a light scattering study

Received: 20 June 2002 / Revised: 5 November 2002 / Accepted: 5 December 2002 / Published online: 15 February 2003


**Abstract** The different mechanisms involved in the aggregation of spherical latex particles coated with bovine serum albumin (BSA) have been studied using static and dynamic light scattering. These techniques assess the fractal dimension of the aggregates and their mean hydrodynamic radius. Particles with different degrees of surface coverage have been prepared. The net charge of the covered particles has been modified by varying the pH of the aqueous phase. The aggregation rate was measured and used to determine the importance of the different aggregation mechanisms that are responsible for these types of flocculation processes. At low and intermediate degrees of surface coverage, bridging flocculation is the principal aggregation mechanism irrespective of the electrical state of the protein-particle complexes. At high degree of surface coverage, however, weak flocculation is important only when the BSA molecules are at their isoelectric point.

**Keywords** Aggregate structure · Bridging flocculation · Dynamic light scattering · Protein adsorption · Static light scattering

## Introduction

Flocculation of protein-coated particles plays an important role in biology and other life sciences. For example, one might think of (1) immunoassays, where antibodies act as flocculating agents for antigen-covered particles and vice versa (Miraballes-Martínez et al. 1996; Ortega-Vinuesa et al. 1996a), and (2) aggregation of micelles which may contain different proteins of biological interest in their membranes (Binks et al. 1989; Merdas et al. 1998; Dimitrova et al. 2000). In these types of processes, the particles may be held together by protein "bridges" which may form between them. Nevertheless, other aggregation mechanisms, such as salt-induced coagulation or weak flocculation, may also be involved. However, it is still not completely clear how the experimental parameters affect the different aggregation mechanisms and the structure of the resulting clusters. Furthermore, the particles may aggregate by more than one aggregation mechanism and so, it might be quite hard to quantify the role of each of them.

Hence, flocculation of protein-coated particles is a highly complex process that shows some analogies with the so-called "bridging flocculation" (Fleer and Lyklema 1973; Pelssers et al. 1990), but in a strict way it cannot be classified as well. Furthermore, even pure bridging flocculation is not understood as thoroughly as salt-induced coagulation and there are still several aspects of indubitable interest for modern research such as the aggregation kinetics (Adachi et al. 1994; Stoll and Buffle 1996; Adachi and Wada 2000), the influence of the flocculating agent's nature (Dickinson and Euston 1992; Yu and Somasundaran 1996; Otsubo 1999; Smalley et al. 2001), the structure of the formed aggregates (Merdas et al. 1998; Biggs et al. 2000; Glover et al. 2000), and the forces that lead to polymer adsorption and their final conformation (Swenson et al. 1998). For this reason, we focus our attention on the kinetic aspects and the structural properties of the aggregates formed by protein-coated particles. As several authors have stated, very little work has been reported on this subject so far (Adachi and Wada 2000; Biggs et al. 2000).

In this paper, three different aggregation mechanisms will be considered: (1) c*oagulation*, where bonds are formed between two uncovered surface patches of the

A. Schmitt (✉) · J. Callejas-Fernández
Biocolloid and Fluid Physics Group,
Department of Applied Physics
University of Granada, 18071 Granada, Spain
E-mail: schmitt@ugr.es
Tel.: +34-958-246104

M. Tirado-Miranda
Department of Physics
University of Extremadura, 10071 Cáceres, Spain

A. Fernández-Barbero
Complex Fluid Physics Group,
Department of Applied Physics,
University of Almería, 04120 Almería, Spain

colliding particles; (2) w*eak flocculation*, i.e. two covered patches of the surface collide; and (3) pure *bridging flocculation* where the collision of an uncovered part of one particle with the covered part of another particle occurs. In this configuration, a "protein bridge" will form between the particles. Several theoretical models have been developed in order to explain the relationship between the aggregation rate and the degree of surface coverage. The pioneer La Mer model considers bridging flocculation to be the only aggregation mechanism (Gregory 1989). From this, more detailed models were proposed (Ash and Clayfield 1976; Hogg 1984; Moudgil et al. 1987; Molski 1989). All of them account for additional aggregation mechanisms and therefore, may be considered as an extension of the La Mer model. Nevertheless, all of them show the common feature that bridging flocculation is the most efficient aggregation mechanism, independently of the experimental conditions. So, an extended model was proposed which considers an independent collision probability for each aggregation mechanism (Schmitt et al. 1998). It is our purpose to apply this model to our experimental system.

In order to quantify the time evolution of the cluster-size distribution in terms of an aggregation rate constant, the analytical form of the corresponding aggregation kernel has to be known. Since this is not possible a priori, the constant aggregation kernel is widely taken as a first approximation (Herrington and Midmore 1990; Holthoff et al. 1996; Van de Ven and Alince 1996; Puertas et al. 1999; Adachi and Wada 2000; Csempesz 2000). However, the hypothesis of a constant aggregation kernel is a severe constraint and, as several authors have revealed, is not suitable for describing the aggregation of protein-coated particles (Pelssers et al. 1990; Schmitt et al. 1998). However, it may be used for the initial steps of aggregation when only dimers are formed and the aggregation rate constants of larger clusters are still not important. The aggregation rate, $k_s$, as obtained by employing the constant kernel solutions of Smoluchowski's rate equation, can also be used to distinguish the importance of the different mechanisms involved in the aggregation process (Herrington and Midmore 1990; Holthoff et al. 1996; Csempesz 2000). In this work, we focus mainly on this aspect. The structural and kinetic information about the aggregating system, which is necessary for determining the aggregation rate, $k_s$, will be obtained using light scattering methods.

Static light scattering (SLS) will be used to determine the aggregate fractal dimension, $d_f$. From the pioneer works on smoke aggregates (Forrest and Witten 1979) and pure proteins (Feder et al. 1984), $d_f$ has been revealed as a very useful parameter for describing the morphology of the clusters. A small $d_f$ is an indication of ramified structures, whereas a larger one corresponds to more compact clusters. Aggregating proteins show a fractal dimension between 2.2 and 2.5 (Feder et al. 1984; Horne 1987; Shuler et al. 1999).

The kinetics of flocculation processes can be studied using dynamic light scattering (DLS). The experimental accessible quantity in this case is the mean hydrodynamic aggregate radius, $\langle R_h \rangle$. From its time evolution, the homogeneity exponent $\lambda$ can be determined (van Dongen and Ernst 1985). This parameter is defined by the relationship, $k_{ai\ aj} = a^{\lambda} k_{ij}$, where $a$ is a large positive number and $k_{ij}$ is the aggregation rate for clusters of size $i$ and $j$. According to its definition, $\lambda$ is an especially useful parameter since it correlates the aggregation rate of clusters at different size scales and, thus, governs the time evolution of the overall aggregation process. Depending on the sticking probabilities, different growth kinetics and size distributions are obtained. $\lambda$ should take the value 0 for diffusion-limited cluster aggregation (DLCA) and a value between 0.5 and 1 for reaction-limited cluster aggregation (RLCA) (Fernández-Barbero et al. 1996). Despite its importance, $\lambda$ is mainly used to describe salt-induced coagulation, whereas its use to describe bridging flocculation or aggregation between coated particles is scarce.

The experimental system used in this work consists of aqueous suspensions of polystyrene microspheres covered with bovine serum albumin (BSA). BSA was selected because it is one of the most abundant blood proteins, comprising about 55% of total blood proteins (Lee et al. 2002). Different amounts of protein were adsorbed onto the particle surface in order to study the influence of the degree of surface coverage. Generally, a colloidal dispersion may lose its stability by adding salt. In this work, we selected an electrolyte concentration slightly above the one normally found in human blood serum. As we discuss below, this salt concentration is sufficient to impede the flocculation of bare particles, whereas, depending on the pH, aggregation of the covered particles can be enhanced or biased.

The major aim of this report is to show that the aggregation rate, $k_s$, as obtained from combined light scattering techniques, reveals useful information on the flocculation mechanisms of protein-coated particles. In particular, the influence of the protein net charge on the different aggregation mechanisms can be determined. The outline of this paper is as follows. The Materials and methods section gives a brief summary of the employed experimental techniques, experimental systems and the theoretical aspects of the cluster structure, growth kinetics and aggregation models. In the following sections, the experimental results will be exposed and discussed.

## Material and Methods

### Sample preparation

Commercially available BSA (Pentex) was chosen as the adsorbing macromolecule. BSA has its isoelectric point at pH 4.8 and is an acidic protein with a net charge of $-18e$ at pH 7 (Lee et al. 2002). This means that BSA carries a slight positive charge at a pH below 4.8, close to zero at pH 4.8 and a negative charge above its isoelectric point. BSA is a globular protein of ellipsoidal shape. Its size is approximately 1.6 nm x 2.7 nm x 2.7 nm. The protein's state of aggregation was checked by native page electrophoresis. BSA dimers were found as the main unit of the sample, although a smaller fraction of high molecular weight aggregates was also detected. The only

treatment prior to adsorption was a cleaning step by dialysis. The protein was used without further purification. Adsorption of globular proteins from aqueous solution on a solid surface is the net result of several sub-processes (Norde and Zoungrana 1998 and cited references herein): (1) electrostatic interaction due to overlap of the electrical double layer around the charged protein molecule and the charged sorbent surface; (2) steric interaction due to the polymeric components at the sorbent surface that extend into the surrounding aqueous phase; (3) changes in the state of hydration; and (4) rearrangements in the protein structure. Also, the conformation of the BSA molecules affects the adsorption. BSA molecules with less $\alpha$-helical content can adsorb faster than native BSA. Generally, BSA becomes less compact and has less $\alpha$-helical content as the pH is lowered (Kim and Cremer 2001). For the protein adsorption experiment, different amounts of BSA were added to a fixed quantity of buffered colloidal suspension. In order to facilitate adsorption, the pH of the suspension was established near the isoelectric point of the BSA molecules, i.e. at pH 4.8. BSA molecules possess a compact structure when the medium pH coincides with their isoelectric point. This structural organization is partially lost when the protein spreads on the sorbent surface, leading to a net increase of the entropy of the system (Norde and Zoungrana 1998 and cited references therein). This is why maximum adsorption is usually achieved near the isoelectric point of BSA, as other authors have found (Peula-García et al. 1994; Ortega-Vinuesa et at. 1996b). Far from the isoelectric point, lateral intermolecular interactions become important and tend to reduce the adsorbed amounts. The corresponding adsorption isotherm shows the high affinity of BSA. At high BSA concentration, a final plateau was reached which indicates the adsorption of a complete monolayer (Norde et al. 1986; Peula-García et al. 1993). This gave us the possibility to obtain particles with a known degree of surface coverage by simply controlling the amount of added protein. Fig. 1 shows the adsorption isotherm of BSA on polystyrene particles. Samples with 0%, 25%, 50%, 75% and 100% of their surface covered by BSA molecules were selected. In order to study the reversibility of adsorption, the BSA-latex complexes were centrifuged. The supernatants were filtered, using a filter of extremely low protein affinity, and measured spectrophotometrically. No protein was detected in the supernatant and therefore the initially adsorbed amount of BSA remains invariant.

## Flocculation experiments

The flocculation experiments were carried out using aqueous suspensions of polystyrene microspheres with different degrees of surface coverage. The bare particle diameter was $99 \pm 1$ nm and the polydispersity index was $0.09 \pm 0.02$, as determined by photon correlation spectroscopy. The particle surface charge density $\sigma_0$ was measured by conductometric titration and found to be weakly pH dependent (Quesada-Pérez 1999). For example, $\sigma_0 = -3.3\ \mu C/cm^2$ at pH 5. The negative particle charge arises from dissociated sulfate groups on the particle surface. The colloidal stability was estimated by determining the critical coagulation concentration (c.c.c.) from the time evolution of the scattered light intensity. The obtained value was $(0.495 \pm 0.007)$ M KCl. The water used for sample preparation was purified by inverse osmosis using Millipore equipment. Prior to aggregation, the samples were sonicated for 15 min in order to break up any initial clusters, thus guaranteeing monomeric initial conditions. Flocculation was induced by mixing equal amounts of buffered electrolyte solution and particle suspension by means of a Y-shaped mixing device. The final electrolyte concentration was 0.250 M KCl. The initial particle concentration in the reaction vessel was $1.6 \times 10^{10}$ cm$^{-3}$ and the temperature was stabilized at $(25 \pm 1)$ °C. The pH was set to 3.2, 4.8 and 9.0 by low ionic strength acetate and borate buffers, respectively. The ionic strength of the buffers was approximately 2 mM, which is quite sufficient to ensure the desired pH. In any case, the exact pH values were always checked experimentally. Aggregation was monitored simultaneously by DLS and SLS. The particle concentration was chosen so that the scattered light intensity was well above the noise level but did not surpass the limit for multiple scattering. At the selected particle concentration, the aggregation kinetics was fast enough to ensure a reasonable run time.

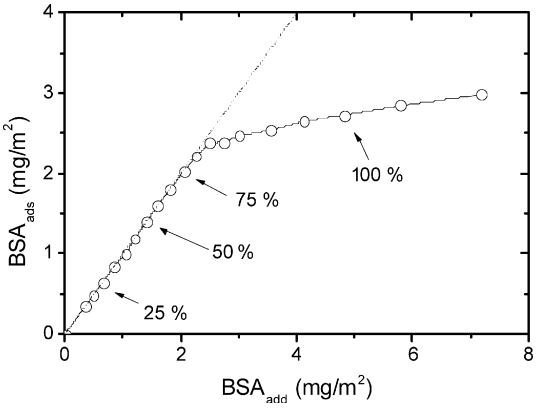


**Fig. 1** Adsorption isotherm of polymeric BSA on latex particles. The pH of the suspension was established near the isoelectric point of the BSA molecules at pH 4.8. The quantities $BSA_{add}$ and $BSA_{ads}$ give the added and adsorbed amount of BSA molecules normalized by the total available particle surface

## Aggregates structure

The morphology of the aggregates was assessed by means of SLS. The light scattering experiments were performed using a slightly modified Malvern 4700 System (UK) working with a 488 nm wavelength argon laser. The photomultiplier arm was previously located at the reference position in order to set the 0° angle. After that, the mean scattered intensity was obtained for different angles in the range from 20° to 140°. SLS allows the fractal dimension, $d_f$, to be measured using the following relationship between the mean scattered light intensity, $I(q)$, and the scattering wave vector, $q = 4\pi/\lambda \sin(\theta/2)$, where $\lambda$ is the medium wavelength and $\theta$ is the scattering angle (Jullien and Botet 1987):

$$I(q) \propto q^{-d_f} \tag{1}$$

The mean scattered intensity contains information about the cluster structure in the $q$ range $< R_h >^{-1} < q < R_0^{-1}$, where $R_0$ is the particle radius. For higher $q$ values the length scale corresponds to individual spheres contained within the clusters, and thus the intensity is related to the particle form factor. In the lower $q$ region, topological length correlations between clusters could be studied. After a sufficiently long time, the mean intensity $I(q)$ showed the expected asymptotic time-independent behaviour for all experiments reported in this paper. This means that the final fractal structure of the clusters was then totally established. From the slope of the asymptotic curves, the fractal dimensions were finally determined (Asnaghi et al. 1992).

## DLS measurements

During DLS measurements, the scattered intensity autocorrelation function is determined from the product of the photon counts at times $t$ and $(t+\tau)$ such that $G(\tau) = < I(t) I(t+\tau) >$. Then, the normalized intensity autocorrelation function:

$$g^{int}(\tau) = \frac{< I(t)\, I(t+\tau) >}{< I(t)\, I(t) >} \tag{2}$$

was calculated and converted into the scattered field autocorrelation function by the aid of the Siegert relationship:

$$g^{\text{int}}(\tau) = 1 + C\left|g^{\text{field}}(\tau)\right|^2 \quad (3)$$

where $C$ is a constant which depends on the optics of the instrument (Pecora 1985).

For our experiments, the scattering angle was set to 60° and the scattered light intensity autocorrelation functions were determined at different times during aggregation. Data analysis was performed using our own programs. Information on the cluster size distribution was obtained from the fitting coefficients of the expanded logarithm of the field autocorrelation function (Koppel 1972):

$$\ln\ g^{field}(\tau) = -\mu_1\tau + \mu_2\left(\frac{\tau^2}{2}\right) + \mu_3\left(\frac{\tau^3}{3!}\right) + \ldots \quad (4)$$

This method is known as cumulant analysis and has been widely used for DLS data analysis. For polydisperse systems, the first cumulant, $\mu_1$, is related to the mean particle diffusion coefficient, $< D >$, by $\mu_1 = < D > q^2$. From the mean particle diffusion coefficient the mean hydrodynamic size may be calculated using the Stokes-Einstein relationship. In order to ensure that the contribution of rotational diffusion can be neglected, the angular dependence of the first cumulant was determined. As an example, Fig. 2 shows $\mu_1$ as a function of $q^2$ for sample pH = 4.8 and $\theta = 0\%$. At all aggregation times, straight lines appear and $\mu_1$ tends to zero as $q \to 0$. This is the expected behaviour for pure translational detection (Tirado-Miranda et al. 1999).

## Aggregation kinetics

The kinetics of aggregation processes in colloidal suspensions may be described by the time evolution of the cluster size distribution, $N_n(t)$, where $n$ is the number of particles contained within the cluster. For dilute colloidal systems, where only binary collisions have to be taken into account, Smoluchowski (1917) proposed the following system of rate equations:

$$\frac{dN_n}{dt} = \frac{1}{2}\sum_{i+j=n} k_{ij}N_iN_j - N_n\sum_{k=1}^{\infty} k_{nk}N_k \quad (5)$$

The aggregation kernel, $k_{ij}$, quantifies the rate at which two clusters of size $i$ and $j$ react and form a cluster of size $i+j$. $k_{ij}$ contains all the physical information about the aggregating system and may be interpreted in terms of a sticking probability for two clusters diffusing towards one another. Analytical solutions of Eq. 5 exist only for a reduced number of kernels such as the constant kernel, the sum kernel, the product kernel and combinations thereof (Odriozola-Prego et al. 1999). The constant kernel, i.e. $k_{ij} = k_s = cte$, implies that the aggregation rate is size independent. It has been used as a reasonable approximation for the DLCA regime in which the aggregates diffuse by pure Brownian motion and, once two clusters collide, they always aggregate. For long times and large clusters, the cluster-size distribution exhibits dynamic scaling and approaches the limiting form (Jullien and Botet 1985):

$$N_n(t) \propto s^{-2}\phi\left(\frac{n}{s}\right) \quad (6)$$

where $s = s(t)$ is related to some average cluster size. $\phi(n/s)$ is a universal time-independent cluster-size distribution, which characterizes the aggregation mechanism. Dynamic scaling implies that the relative shape of the cluster-size distribution remains constant during the whole aggregation process. Considering the dynamic scaling solution (Eq. 6) and the fractal cluster morphology, the mean hydrodynamic radius of the aggregates, $< R_h(t) >$, can be expressed as:

$$\langle R_h(t)\rangle = R_0 t^{\frac{1}{d_f(1-\lambda)}} \quad (7)$$

This relationship can be used to determine $\lambda$ from the experimental time evolution of mean hydrodynamic cluster radius, once $d_f$ is known (Ziff 1984).

## Aggregation mechanism

In order to analyse the data in detail, one should take into account that the aggregation probability for a colliding pair of colloidal particles depends also on whether the colliding part of the surface is covered by protein or not. The probability of finding a covered surface patch is given by the fractional surface coverage, $\theta$, and the probability of finding a bare part by $(1-\theta)$. Hence, $(1-\theta)^2$ gives the probability that two particles collide in *coagulation* configuration, i.e. with the bare parts of their respective surfaces. The aggregation rate for this configuration will be denoted $k_c$. *Weak flocculation*, i.e. the aggregation of two covered surface patches, corresponds to $\theta^2$, and in this case the aggregation rate is denoted $k_{wf}$. For bridging flocculation, stable bonds are formed between a covered surface patch of one particle and an uncovered patch of another one. Thus, the aggregation rate should be proportional to the number of free sites on one particle and also to the number of occupied sites on the other one. Consequently, the corresponding aggregation rate, $k_{bf}$, should be multiplied by $\theta(1-\theta)$. This relationship implies that bridging flocculation is most effective at half surface coverage.

According to the model proposed by Schmitt et al. (1998), the total aggregation rate may be written as the sum of all contributions:

$$k_s(\theta) = k_c(1-\theta)^2 + k_{wf}\theta^2 + 2k_{bf}\theta(1-\theta) \quad (8)$$

where the factor of 2 is introduced in order to account for the two possible bridging configurations: the collision of an uncovered part of one particle with the covered part of another particle and the reverse case. This relationship allows the contribution of the different aggregation mechanisms to be quantified if the aggregation rate, $k_s$, is known as a function of the degree of surface coverage, $\theta$.

Using the dynamic scaling solution (Eq. 6) and the constant kernel approximation for the time evolution of the cluster-size distribution, the following relation for the first cumulant of the field autocorrelation function has been obtained (Olivier and Sorensen 1990):

$$\mu_1(t) = \mu_1(0)\left(1 + \frac{t}{t_{agg}}\right)^{\frac{-1}{d_f(1-\lambda)}} \quad (9)$$

where $t_{agg} = 2/c_0k_s$ is the characteristic aggregation time. $t_{agg}$ is expressed as a function of the initial particle concentration, $c_0$, and the Smoluchowski rate constant, $k_s$. Equation 9 allows the characteristic aggregation time, $t_{agg}$, to be obtained once $d_f$ and $\lambda$ are known. $k_s$ can then be determined from $t_{agg}$ using the known initial particle concentration (Tirado-Miranda et al. 1998).

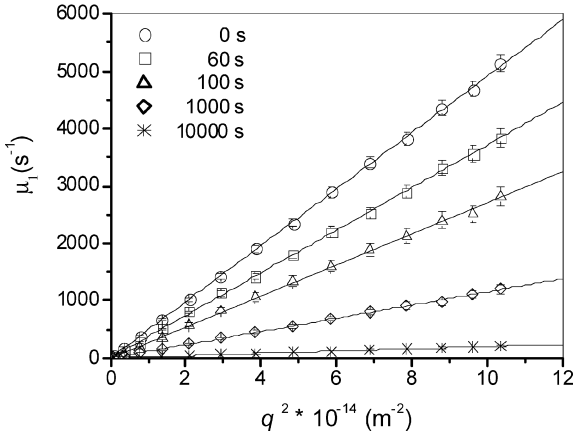


**Fig. 2** Angular dependence of the first cumulant at different times for pH = 4.8 and $\theta = 0\%$

## Results

Using Eq. 1, the cluster fractal dimension, $d_f$, was obtained by measuring the mean scattered light intensity, $I$, as a function of the scattering vector, $q$. Figure 3 shows a typical plot for the time evolution of the mean intensity. It can clearly be seen that this function tends towards a limiting long-time behaviour, from which the cluster fractal dimension can be easily obtained. Obviously, a longer time is required for reaching this asymptotic curve in the low-$q$ range, corresponding to the larger structures. For higher $q$ values, the final curve is observed almost from the beginning, when only small clusters are present. Examining the curves in more detail, one might think that the slope increases from about $-1.4$ to a final value of approximately $-2$, and so $d_f$ seems to be time dependent. Nevertheless, this apparent increase is still due to the decreasing curvature of the $I(q)$ curves rather than a change in the fractal structure of the aggregates. As can be seen in Fig. 3, the curves with a slope smaller than approximately $-2$ are still slightly bent and it is not possible to fit a well-defined straight line to them. Hence, the curves are still affected by the limited cluster size, i.e. the clusters are still too small so that the lack of self-similarity at large length scales (small $q$ values) affects the $I(q)$ curves at short length scales (large $q$ values). Consequently, the fractal dimension $d_f$ can be reliably obtained only at very large aggregation times when the $I(q)$ curves show the expected linear behaviour over a sufficiently large $q$ range. This, however, does not imply that the fractal structure of the smaller aggregates is changing in time or not well defined. It is only not yet observable. Table 1 contains the obtained fractal dimensions. Excluding the sample for $\theta = 25\%$ at pH 3.2, where $d_f = 1.9$, all observed values are closer to 2.1, which is the commonly accepted value for RLCA processes.

Time-resolved DLS was employed for monitoring the average diffusion coefficient of the aggregates. The average hydrodynamic radius, $< R_h >$, was calculated using the Einstein-Stokes equation. In Fig. 4, the time evolution of $< R_h >$ is plotted in logarithmic scale for two different samples. In all cases, the data align on a straight line, even for quite small clusters. The observed power law is characteristic for dynamic scaling and in good agreement with the theoretical prediction given by Eq. 7. It should be pointed out that the exponential behaviour, predicted for RLCA and $\lambda = 1$, could not be observed. The curves always rise, describing a power law almost from the beginning. This implies that the cluster size distribution may be described by the dynamic scal-

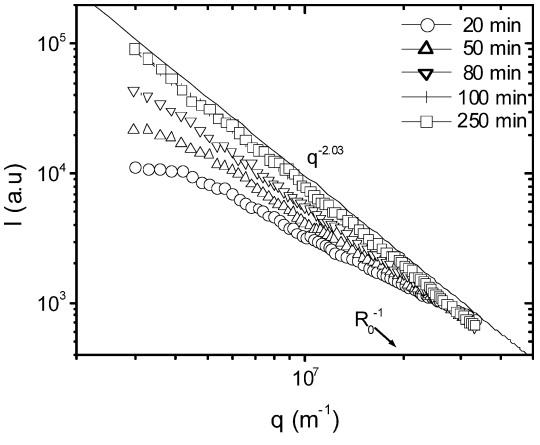


**Fig. 3** Time evolution of the scattered light intensity as a function of the scattering vector for pH = 4.8 and $\theta = 0\%$

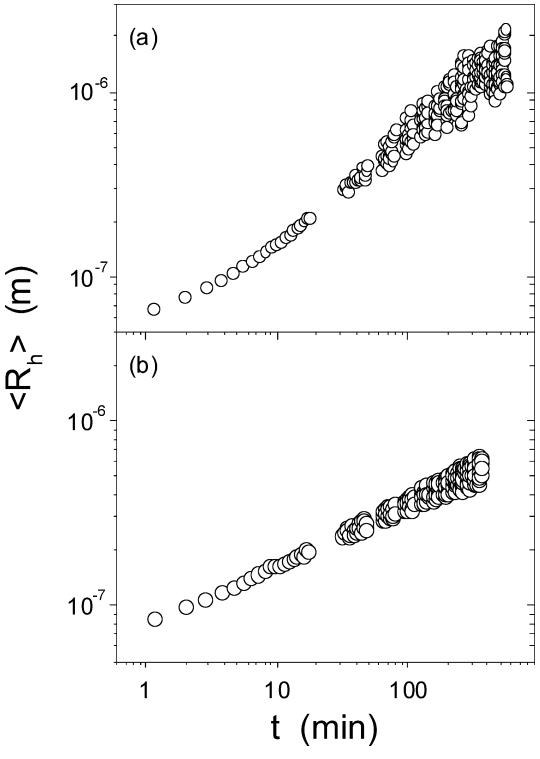


**Fig. 4** Average hydrodynamic radius as a function of time for: (**a**) pH = 9.0 and $\theta = 25\%$, at which $\lambda > 0$, and (**b**) pH = 3.2 and $\theta = 50\%$, at which $\lambda < 0$

**Table 1** Fractal dimension, $d_f$, and homogeneity exponent, $\lambda$, as a function of the degree of surface coverage, $\theta$, obtained at three different pH values

| $\theta$(%) | pH 3.2 | | pH 4.8 | | pH 9.0 | |
|---|---|---|---|---|---|---|
| | $d_f$ | $\lambda$ | $d_f$ | $\lambda$ | $d_f$ | $\lambda$ |
| 0 | $2.17 \pm 0.03$ | $0.43 \pm 0.02$ | $2.03 \pm 0.03$ | $0.33 \pm 0.02$ | $2.19 \pm 0.03$ | $0.42 \pm 0.02$ |
| 25 | $1.92 \pm 0.03$ | $-0.15 \pm 0.02$ | $2.23 \pm 0.03$ | $-0.10 \pm 0.01$ | $2.29 \pm 0.03$ | $0.28 \pm 0.03$ |
| 50 | $2.24 \pm 0.03$ | $-0.31 \pm 0.03$ | $2.27 \pm 0.03$ | $-0.26 \pm 0.03$ | – | – |
| 75 | – | – | $2.33 \pm 0.04$ | $-0.18 \pm 0.02$ | – | – |
| 100 | – | – | $2.39 \pm 0.04$ | $-0.12 \pm 0.01$ | – | – |

ing approach practically for the whole aggregation process and, even for the early aggregation stages, the dynamic scaling solution is at least a good approximation. Using the fractal dimension as obtained from the independent SLS experiments, $\lambda$ was determined by fitting the experimental data according to Eq. 7. The obtained results are summarized in Table 1.

Once $d_f$ and $\lambda$ were known, Eq. 9 was then employed for obtaining the characteristic aggregation time, $t_{agg}$, and there from the Smoluchowski rate constant, $k_s$. For this purpose the first cumulant, $\mu_1$, was plotted as a function of the scaled time, $1 + t/t_{agg}$. The characteristic aggregation, $t_{agg}$, was then varied until all experimental points aligned, according to Eq. 9, on a straight line with a slope of unity (see Fig. 5). The Smoluchowski rate constant, $k_s$, was calculated from the obtained $t_{agg}$ values using the known initial particle concentration. Figure 6 shows the experimentally obtained $k_s$ values as a function of the degree of surface coverage at the three different pH values used in this study. The best fits according to Eq. 8 are also included in the plots. The corresponding fitting parameters are given in Table 2.

## Discussion

The measured fractal dimensions surpass in almost all cases the value of 2. This indicates that relatively compact structures are formed. Similar values were obtained for processes involving pure bridging flocculation (Glover et al. 2000) or bare protein aggregation (Horne 1987; Shüler et al. 1999). At pH 4.8, we observe that the fractal dimension rises for increasing surface coverage, i.e. the aggregates tend to become more compact. A similar behaviour has been observed before for other experimental systems (Tirado-Miranda et al. 1999). In that case, the authors found that the fractal dimension rose from $d_f = 1.74$ for clusters formed by aggregating bare particles up to 2.7 for sodium dodecyl sulfate (SDS)-covered particles. This dramatic increase in $d_f$ was explained taking into account that osmotic and elastic-steric interactions lower the binding strength and, thus, allow for internal rearrangement processes once the clusters are formed. In our experimental systems, however, the bare particles aggregate at an electrolyte concentration of 0.250 M, which is insufficient for ensuring a diffusion-limited aggregation regime. Nevertheless, even in this case the fractal dimension tends to increase for increasing surface coverage. This indicates that the adsorbed protein layer plays a similar role as the SDS layer in the aforementioned experiments, and so, osmotic and elastic-steric interactions may be evoked for explaining the observed behaviour.

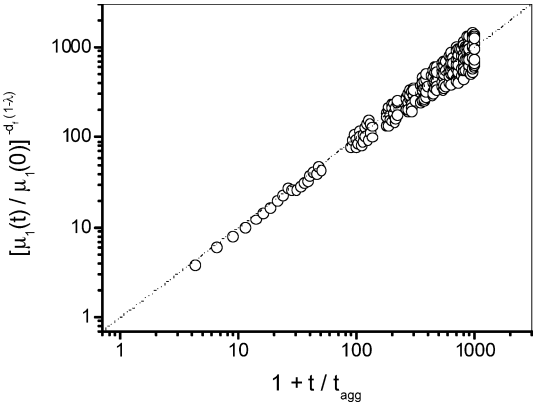


**Fig. 5** Time evolution of the normalized first cumulant as a function of the scaled time for pH = 3.2 and $\theta = 50\%$

**Table 2** Aggregation rate constants $k_c$, $k_{wf}$ and $k_{bf}$ obtained at three different pH values

| pH | $k_c$ ($10^{-12}$ cm$^3$ s$^{-1}$) | $k_{wf}$ ($10^{-12}$ cm$^3$ s$^{-1}$) | $k_{bf}$ ($10^{-12}$ cm$^3$ s$^{-1}$) |
|---|---|---|---|
| 3.2 | $1.8 \pm 2.3$ | $0.0 \pm 2.6$ | $9.4 \pm 3.6$ |
| 4.8 | $1.2 \pm 0.8$ | $4.9 \pm 0.8$ | $10.5 \pm 1.5$ |
| 9.0 | $0.8 \pm 0.3$ | $0.0 \pm 0.3$ | $0.6 \pm 0.4$ |

The aggregation kinetics will be discussed mainly in terms of two parameters, the obtained homogeneity exponent, $\lambda$, and the Smoluchowski aggregation rate, $k_s$. Prior to a more detailed discussion, however, it should be pointed out that negative values were found for $\lambda$. Although the van Dongen-Ernst theory does not forbid those values, it is difficult to find them in the literature (Delgado-Calvo-Flores 2000; Molina-Bolivar et al. 2001; Tirado-Miranda 2001). According to its definition, the physical meaning of negative $\lambda$ values is that the small cluster-small cluster union is favoured and more likely than the aggregation of larger clusters. This implies that the aggregation rate should slow down as the aggregation processes go on. This behaviour was clearly observed in our data (comparing Fig. 4a and b) and thus supports the obtained negative $\lambda$ values.

Before we enter the detailed discussion for the different pH values, it is convenient to compare briefly the results obtained for bare particles. According to Table 1, the aggregation processes seem to be pH independent. In all cases, similar values for both $d_f$ and $\lambda$ are obtained. The $\lambda$ values between 0.3 and 0.4 point towards relatively slow aggregation kinetics, which implies that the clusters collide more than once prior to aggregation. The values found for the fractal dimension, $d_f$, are very close to the ones found for RLCA processes, which indicates that relatively compact structures are formed. Consequently, the fast aggregating DLCA regime is not achieved and so the screening of the particle surface charge is not complete. From the point of view of the interaction energy picture according to the DLVO theory, we conclude that the repulsive energy barrier does still exist, although it is lowered considerably.

### At pH = 3.2

At this pH, the latex particles are negatively charged whereas the BSA molecules bear a positive net charge.

Here, we find aggregation at the intermediate range of surface coverage for $\theta = 25$–$50\%$. At $\theta = 25\%$, the fractal dimension, $d_f = 1.92$, is smaller than the corresponding one at $\theta = 50\%$. Furthermore, the homogeneity exponent $\lambda$ is negative and its absolute value is also smaller than the one obtained at $\theta = 50\%$. These data imply that rather small and ramified aggregates are formed. For relatively low degrees of coverage, we may assume that there are surface patches carrying a local positive charge arising from the BSA molecules and areas of unoccupied surface still bearing the original particle charge. So, in a microscopic analysis, two particles may collide with positive and negative areas of their respective surface, giving rise to bond formation due to electrical attraction. This process can be seen as a kind of charge-mediated flocculation in which the protein molecules act as "bridges" between the aggregating particles. Nevertheless, we cannot exclude the possibility that the particles join through unoccupied patches of their respective surfaces, i.e. that also coagulation takes place. At a larger scale, the protein-particle complexes may be considered to act as homogeneously charged spheres. From this point of view, aggregation is generally favoured since the net charge of the covered particles and, consequently, the electrostatic repulsion term for the total DLVO interaction energy are smaller than the ones for the uncovered particles.

The situation is quite different at high degrees of surface coverage, $\theta = 75$–$100\%$, where aggregation practically does not take place. Here, two mechanisms prevent aggregate formation. The first one is related to the fact that practically all surface patches carry locally a positive net charge, which will always give rise to a repulsive energy barrier between two colliding particles. The second one is due to repulsive steric interactions which arise when two layers of adsorbed proteins come into contact (Tirado-Miranda et al. 1999).

As can be seen in Fig. 6, the corresponding $k_s$ versus $\theta$ curve is roughly "bell shaped", which indicates that bridging flocculation is the main aggregation mechanism. Fitting the curve according to Eq. 8 allows us to quantify the weight of the different aggregation mechanisms. The obtained fitting parameters are summarized in Table 2. They show that weak flocculation is not observed whereas protein bridging is about five times as effective as pure coagulation. This means that, at pH 3.2, the aggregation kinetics is almost completely controlled by "protein bridging". This can be illustrated at the relatively low degree of surface coverage of $\theta = 25\%$. In this case, the probability for two approaching particles to collide with their bare surface patches is given by $(1-\theta)^2 = 56\%$, while the probability for particle encounters in bridging configuration is only $2\theta(1-\theta) = 38\%$. Hence, one expects the aggregation process to be mainly governed by pure coagulation. However, the contribution of pure coagulation to the overall aggregation rate, $k_c(1-\theta)^2 = 1.0\times10^{-12}$ cm$^3$/s, is more than three times smaller than the contribution of bridging flocculation, $2k_{bf}\theta(1-\theta) = 3.5\times10^{-12}$ cm$^3$/s. This

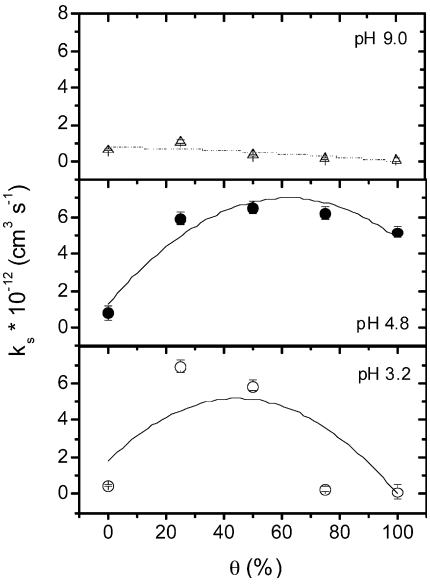


**Fig. 6** Smoluchowski rate constant, $k_s$, versus degree of surface coverage for pH = 3.2, 4,8 and 9.0, respectively. The *data points* were obtained averaging over three independent measurements. The *error bars* give the statistical error of the mean value. The lines show the best fit according to Eq. 8

means that aggregation occurs mainly in bridging configuration and the probability for bridging flocculation is so high that it overcompensates the lower collision probability for this mechanism at low degrees of surface coverage.

At pH = 4.8

At this pH, aggregation is observed to a greater or lesser extent at all degrees of surface coverage (see Fig. 6). Here, the latex particles are negatively charged whereas the BSA molecules are at their isoelectric point. For low surface coverage, there should be negative and electrically uncharged areas on the particle surface. Hence bridging flocculation becomes possible when uncharged and negative areas of different particles come into contact. This mechanism is based on the high affinity of electrically uncharged BSA molecules for the negatively charged surface, i.e. the binding forces for this aggregation mechanism seem to be very similar to the interaction which enables the isolated protein molecules to adsorb onto the bare particle surface. As can be seen in Table 2, coagulation between uncoated surface patches of colliding particles still occurs, although at a relatively low rate which is about 10 times smaller than the rate for pure bridging flocculation. The explanation for the non-vanishing aggregation rate at low degrees of surface coverage is quite similar to the one given for pH 3.2, i.e. the electrolyte concentration is high enough to decrease the height of the repulsive energy barrier so that pure aggregation becomes possible. However, it is insufficient to screen

the particle net charge completely and thus, only a relatively reduced aggregation rate is achieved.

At high degrees of surface coverage, one expects steric repulsion to impede weak flocculation since the covered surface patches of one particle will not find free space on another one. Nevertheless, the aggregation rate for completely covered particles reaches almost half the value observed for pure bridging flocculation (see Table 2). This may be understood if one supposes that the adsorbed layer of neutral protein molecules reduces the long-range repulsive electrostatic interactions between two approaching particles. According to Elgersma et al (1990), this is possible since adsorption of neutral protein molecules may lead to entropically driven counter-ion rearrangement and thus, lower the particle net charge. This idea was corroborated by Peula-García et al. (1994) and Ortega-Vinuesa et al. (1996b), who measured the electrophoretic mobility of protein-covered latex particles. Their results showed that the electrophoretic mobility decreases for an increasing amount of adsorbed protein.

At pH = 9.0

At high pH, slow but significant aggregation is observed only for $\theta = 0\%$ and 25%. In both cases, the experimental data indicate that the small cluster-small cluster union is biased ($\lambda > 0$; see Table 1). As was explained before, the latex particles and the BSA molecules bear negative net charge at high pH. This means that the electrostatic repulsion is enhanced for increasing degrees of surface coverage and finally, becomes so high that it impedes flocculation almost completely. This explains why only pure coagulation and some bridging flocculation at low degrees of surface coverage are still possible.

## Conclusions

In summary, we studied the flocculation mechanism of protein-coated particles under conditions usually found in biological systems. The fractal dimensions obtained by SLS show that relatively compact structures are formed. Combining these results with DLS data we found negative values for $\lambda$, which indicates that, in these cases, the small cluster-small cluster union is favoured and more likely than the aggregation of larger clusters. Irrespective of the electrical state of the protein-particle complexes, bridging flocculation is the main aggregation mechanism at both low and intermediate degrees of protein coverage. Weak flocculation is important at high degrees of coverage only if the adsorbed BSA molecules are at their isoelectric point.

**Acknowledgements** This work was supported by "Ministerio de Ciencia y Tecnología, Plan Nacional de Investigación, Desarrollo e Innovación Tecnológica (I + D + I)", project nr. MAT2000-C03-01, -02 and -03. We also wish to express gratitude to Dr. Manuel Quesada-Pérez for latex particle characterization.

## References

Adachi Y, Wada T (2000) Initial stage of bridging flocculation of polystyrene latex spheres with polyethylene oxide. J Colloid Interface Sci 229:148–154

Adachi Y, Cohen-Stuart MA, Fokkink R (1994) Dynamic aspects of bridging flocculation studied using standardized mixing. J Colloid Interface Sci 167:346–351

Ash SG, Clayfield EJ (1976) Effect of polymers on the stability of colloids. Flocculation of polystyrene latex by polyethers. J Colloid Interface Sci 55:645–657

Asnaghi D, Carpineti M, Giglio M, Sozzi M (1992) Coagulation kinetics and aggregate morphology in the intermediate regimes between diffusion limited and reaction limited cluster aggregation. Phys Rev A 45:1018–1023

Biggs S, Habgood M, Jameson GJ, Yan Y (2000) Aggregate structures formed via a bridging flocculation mechanism. Chem Eng J 80:13–22

Binks BP, Chatenay D, Nicot C, Urbach W, Waks M (1989) Structural parameters of the myelin transmembrane proteolipid in reverse micelles. Biophys J 55:949–955

Csempesz F (2000) Enhanced flocculation of colloidal dispersions by polymer mixtures. Chem Eng J 80:43–49

Delgado-Calvo-Flores JM (2000) PhD thesis, University of Granada, Spain

Dickinson E, Euston S (1992) Short-range structure of simulated flocs of particles with bridging polymer. Colloids Surf 62:231–242

Dimitrova M, Tsekov R, Matsumura H, Furusawa K (2000) Size dependence of protein-induced flocculation of phosphatidylcholine liposomes. J Colloid Interface Sci 226:44–50

Elgersma AV, Zsom RLJ, Norde W, Lyklema J (1990) The adsorption of bovine serum albumin on positively and negatively charged polystyrene latices. J Colloid Interface Sci 138:145–156

Feder J, Jossang T, Rosenquist E (1984) Scaling behavior and cluster fractal dimension determined by light scattering from aggregating proteins. Phys Rev Lett 53:1403–1406

Fernández-Barbero A, Cabrerizo-Vílchez MA, Martínez-García R, Hidalgo-Álvarez R (1996) Effect of the particle surface charge density on the colloidal aggregation mechanism. Phys Rev E 53:4981–4989

Fleer GF, Lyklema J (1973) Polymer adsorption and its effects on the stability of hydrophobic colloids. II. The flocculation process as studied with the silver iodide-polyvinyl alcohol system. J Colloid Interface Sci 46:1–12

Forrest SR, Witten TA Jr (1979) Long-range correlations in smoke-particle aggregates. J Phys A 12:L109–L117

Glover SM, Yan Y, Jameson GJ, Biggs S (2000) Bridging flocculation studied by light scattering and settling. Chem Eng J 80:3–12

Gregory J (1989) Fundamentals of flocculation. Crit Rev Env Control 19:185–230

Herrington TM, Midmore BR (1990) Determination of an average rate constant for the rapid coagulation of polydisperse suspension using photon correlation spectroscopy. J Chem Soc Faraday Trans 86:671–674

Hogg RJ (1984) Collision efficiency factors for polymer flocculation. J Colloid Interface Sci 102:232–236

Holthoff H, Egelhaaf S, Borkovec M, Schurtenberger P, Sticher H (1996) Coagulation rate measurements of colloidal particles by simultaneous static and dynamic light scattering. Langmuir 12:5541–5549

Horne DS (1987) Determination of the fractal dimension using turbidimetric techniques. Faraday Discuss Chem Soc 83:259–270

Jullien R, Botet R (1987) Aggregation and fractal aggregates. World Scientific, River Edge, NJ, USA

Kim J, Cremer PS (2001) Elucidating changes in interfacial water structure upon protein adsorption. Chem Phys Chem 8/9:543–546

Koppel DEJ (1972) Analysis of macromolecular polydispersity in intensity correlation spectroscopy: the method of cumulants. J Chem Phys 57:4814–4820

Lee WK, Ko JS, Kim HM (2002) Effect of electrostatic interaction of globular proteins on octacalcium phosphate crystal film. J Colloid Interface Sci 246:70–77

Merdas A, Gindre M, Le Huérou JY, Nicot C, Ober R, Urbach W, Waks M (1998) Bridging of nonionic reverse micelles by a myelin transmembrane protein. J Phys Chem B 102:528–533

Miraballes-Martínez I, Martín-Rodríguez A, Hidalgo-Álvarez R (1996) Strategies to improve the colloidal stability and the reactivity of immunolatex beads. J Disper Sci Technol 17:321–337

Molina-Bolivar JA, Galisteo-Gonzalez F, Hidalgo-Alvarez R (2001) Fractal aggregates induced by antigen-antibody interaction. Langmuir 17:2514–2520

Molski A (1989) On the collision efficiency approach to flocculation. Colloid Polym Sci 267:371–375

Moudgil BM, Shah BD, Soto HS (1987) Collision efficiency factors in polymer flocculation of fine particles. J Colloid Interface Sci 119:466–473

Norde W, Zoungrana T (1998) Surface-induced changes in the structure and activity of enzymes physically immobilized at solid/liquid interfaces. Biotechnol Appl Biochem 28:133–143

Norde W, Macritchie F, Nowicka G, Lyklema J (1986) Protein adsorption at solid liquid interfaces: reversibility and conformation aspects. J Colloid Interface Sci 112:447–456

Odriozola G, Schmitt A, Callejas-Fernández J, Martínez-García R, Hidalgo-Álvarez R (1999) Dynamic scaling concepts applied to numerical solutions of Smoluchowski's rate equation. J Chem Phys 111:7657–7667

Olivier BJ, Sorensen CM (1990) Evolution of the cluster size distribution during slow colloid aggregation. J Colloid Interface Sci 134:139–146

Ortega-Vinuesa JL, Molina-Bolívar JA, Hidalgo-Álvarez R (1996a) Particle enhanced imunoaggregation of $F(ab')_2$ molecules. J Immunol Methods 190:29–38

Ortega-Vinuesa JL, Gálvez-Ruiz, MJ, Hidalgo-Álvarez R (1996b) $F(ab')_2$-coated polymers carriers: electrokinetic behavior and colloidal stability. Langmuir 12:3211–3220

Otsubo Y (1999) Rheological behavior of suspensions flocculated by weak bridging of polymer coils. J Colloid Interface Sci 215:99–105

Pecora R (1985) Dynamic light scattering. Plenum Press, New York

Pelssers EGM, Cohen-Stuart MA, Fleer GJ (1990) Kinetics of bridging flocculation. Role of relaxations in the polymer layer. J Chem Soc Faraday Trans 86:1355–1361

Peula-García JM, de las Nieves-López FJ (1993) Adsorption of monomeric bovine serum albumin on sulfonated polystyrene model colloids. I. Adsorption isotherms and effect of the surface charge density. Colloids Surf A 77:199–208

Peula-García JM, Callejas-Fernández J, de las Nieves-López FJ (1994) Adsorption of monomeric bovine serum albumin on sulfonated polystyrene model colloids. II. Electrokinetic characterization of latex-protein complexes. In: West R, Batts G (eds) Surface properties of biomaterials. Butterworth-Heinemann, London, pp 61–69

Puertas AM, Maroto JA, Fernández-Barbero A, de las Nieves FJ (1999) Particle interactions in colloidal aggregation by Brownian dynamics simulation. Phys Rew E 59:1943–1947

Quesada-Pérez M (1999) PhD thesis, University of Granada, Spain

Schmitt A, Fernández-Barbero A, Cabrerizo-Vílchez MA, Hidalgo-Alvarez R (1998) On the identification of bridging flocculation: an extended collision efficiency model. Prog Colloid Polym Sci 110:105–109

Schüler J, Frank J, Saenger W, Georgalis Y (1999) Thermally induced aggregation of human transferrin receptor studied by light scattering techniques. Biophys J 77:1117–1125

Smalley MV, Hatharasinghe HLM, Osborne I, Swenson J, King SM (2001) Bridging flocculation in vermiculite-peo mixtures. Langmuir 17:3800–3812

Smoluchowski MV (1917) Versuch einer mathematischen Theorie der Koagulationskinetik kolloider Lösungen. Z Phys Chem 92:129

Stoll S, Buffle J (1996) Computer simulation of bridging flocculation processes: the role of colloid to polymer concentration ratio on aggregation kinetics. J Colloid Interface Sci 180:548–563

Swenson J, Smalley MV, Hatharasinghe HLM (1998) Mechanism and strength of polymer bridging flocculation. Phys Rev Lett 81:5840–5843

Tirado-Miranda, M (2001) PhD thesis, University of Granada, Spain

Tirado-Miranda M, Schmitt A, Callejas-Fernández J, Fernández-Barbero A (1998) Experimental evidence of rearrangement in fractal clusters. Prog Colloid Polym Sci 110:110–113

Tirado-Miranda M, Schmitt A, Callejas-Fernandez J, Fernandez-Barbero A (1999) Colloidal clusters with finite binding energies: fractal structure and growth mechanism. Langmuir 15:3437–3444

Van de Ven TG, Alince B (1996) Heteroflocculation by asymmetric polymer bridging. J Colloid Interface Sci 181:73–78

Van Dongen PGJ, Ernst MH (1985) Dynamic scaling in the kinetics of clustering. Phys Rev Lett 54:1396–1399

Yu X, Somasundaran P (1996) Role of polymer conformation in interparticle-bridging dominated flocculation. J Colloid Interface Sci 177:283–287

Ziff RM (1984) Kinetics of aggregation and gelation. North-Holland, Amsterdam